Journal of Analytical and Applied Pyrolysis 172 (2023) 105994

Contents lists available at ScienceDirect

Journal of Analytical and Applied Pyrolysis

journal homepage: www.elsevier.com/locate/jaap

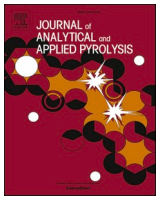

Low- and high-molecular weight fractions of geological ambers detected by evolved gas analysis-mass spectrometry

Marco Mattonai [a,*], Lucia Andrei [a], Marian Vîrgolici [b], Erika Ribechini [a]

[a] Department of Chemistry and Industrial Chemistry, University of Pisa, Via Giuseppe Moruzzi 13, 56124 Pisa, Italy
[b] "Horia Hulubei" National Institute of Physics and Nuclear Engineering, 30, Reactorului Street, Magurele, Ilfov, Romania

ARTICLE INFO

Keywords:
Amber
Evolved gas analysis
Mass spectrometry
Terpenoids
Succinite

ABSTRACT

We used evolved gas analysis-mass spectrometry (EGA-MS) to characterize a pool of ambers belonging to different geological varieties, with the aim of obtaining information on both their non-polymeric and polymeric components. Small molecular components can be trapped in amber during the fossilization process. Their characterization can provide insights into the maturation process of amber and help in determining its age and botanical origin. Most of the analyzed ambers showed two gas evolution regions, corresponding to the desorption of low-molecular weight compounds at low temperature, and to the pyrolysis of the macromolecular matrix at high temperature. We established characteristic *m/z* signals of the non-polymeric and polymeric fractions, and we were able to classify most of the samples in agreement with the available literature. We also performed principal component analysis of diterpenoid ambers using their average mass spectra. This allowed us to differentiate between succinite and rumanite ambers, which showed very similar spectra. The results demonstrate that EGA-MS constitutes a reliable technique to obtain information on the molecular composition of ambers, and on their relative content of low- and high-molecular weight fractions.

1. Introduction

Amber is obtained by the fossilization of tree resin on a geological time scale. The fossilization process requires the resin to be incorporated in sediments under specific environmental conditions, such as a low availability of oxygen and closeness to a river delta or lagoon [1]. Such conditions can only be met in few places on the planet, making amber a rare, precious material whose value has been acknowledged since ancient times [2–4]. Fossilization of resin into amber is a complex phenomenon which involves two main processes: polymerization and maturation [5,6]. Polymerization involves the coupling of resin terpenoids, leading to the formation of the bulk macromolecular matrix of amber. This process is relatively fast, and can be even observed in fresh tree resin exposed to air and light. On the other hand, maturation is a slow process which involves isomerization and loss of functional groups [7]. Maturation depends not only on the composition of amber, but also on its geological age and thermal history [8].

As the macromolecular bulk of amber is formed and undergoes maturation, smaller, non-polymeric components of resin can either be lost in the environment, or trapped in the polymeric matrix. In the last decades, studies have shown that ambers at more advanced stages of maturation usually have a lower content of non-polymeric species [7]. Therefore, knowledge of the relative content of the two fractions could provide valuable insights into the degree of maturation of amber, as well as into the reaction pathways involved in the fossilization process. One of the main challenges in obtaining separate information on the molecular and macromolecular fractions of ambers is that they often share similar structural features, as the components of the non-polymeric fraction are the precursors of the polymeric one [9].

Common analytical techniques used to characterize amber are spectroscopies such as FTIR, Raman and NMR [10–13], and thermo-analytical techniques such as TGA and DSC [14,15]. These techniques are used to characterize whole amber samples, and separating the contributions of the molecular and polymeric fractions is extremely challenging. The non-polymeric fraction of amber can be solubilized and characterized by derivatization followed by GC-MS analysis [16] or by SPME [17]. However, this approach can be time-consuming, and often requires considerable amounts of sample, which are not always available. Analytical pyrolysis coupled to GC-MS (Py-GC/MS) is a powerful and widely used technique to characterize amber, providing molecular-level information on both the non-polymeric and polymeric fractions. Py-GC/MS is often carried out

* Corresponding author.
E-mail address: marco.mattonai@dcci.unipi.it (M. Mattonai).

https://doi.org/10.1016/j.jaap.2023.105994
Received 31 January 2023; Received in revised form 21 April 2023; Accepted 2 May 2023
Available online 4 May 2023

using in situ derivatization with a methylating or a silylating agent to improve the chromatographic performances of desorption/pyrolysis products with polar moieties [3,7,18–22]. The pioneering work by Anderson and co-workers with Py-GC/MS led to the establishment of a well-known classification system in which ambers are categorized on the basis of the structure of their polymeric fraction [6]. Pyrolysis temperature in Py-GC/MS experiments can be modulated to either desorb the non-polymeric components and leave the polymeric matrix unaltered, or to pyrolyze the macromolecular bulk [23]. For instance, Anderson and co-workers reported that Py-GC/MS of succinite at different temperatures provided chromatograms containing different sets of terpenoid compounds [18]. Virgolîci and co-workers characterized ambers by thermal desorption-GC/MS, heating the samples at 200 °C to desorb non-polymeric compounds without degrading the macromolecular bulk [24].

Ambers with different chemical compositions can show significantly different thermal behaviors. Establishing the optimal temperature to selectively achieve desorption or pyrolysis through Py-GC/MS requires preliminary studies, which can be very time-intensive and consume significant amounts of sample.

Evolved gas analysis-mass spectrometry (EGA-MS) is a versatile technique that can be used to monitor the evolution of desorption/pyrolysis products from a sample as a function of temperature. EGA-MS shares the advantage of Py-GC/MS of minimal sample preparation, and is often used to study complex samples of both natural and synthetic origin. EGA-MS is also a powerful screening technique to establish the optimal desorption/pyrolysis temperatures before Py-GC/MS analysis [25–28], avoiding the need of preliminary Py-GC/MS experiments at different temperatures. To the best of our knowledge, however, no studies are available in the literature describing the thermal behavior of ambers using EGA-MS.

In the present work, we performed EGA-MS of a pool of geological ambers with different origins, with the aim of obtaining insights into the composition of both the non-polymeric and polymeric fractions of amber and into their thermal behaviors.

2. Materials and methods

2.1. Samples

46 geological ambers were investigated in this study. A list of all samples is provided in Table 1, and photos for some of the samples are available in the Supplementary Material. The ambers were provided by nine different collections belonging to museums and academic institutes. Information on the classification and geographical origins of the samples are listed as provided by the institutes, when available. Eight samples derive from the amber deposit in Bitterfeld, the largest amber reservoir in Germany. Bitterfeld ambers have been dated to the Oligocene period, between 25 and 23 million years ago [12,16,29]. Three samples derive from different locations of the Pomeranian Voivodeship, including Gdansk and Mikoszewo. Ambers from the Baltic shores have also been dated to either Eocene or Oligocene [14,30]. All rumanite samples derive from the basins in Colti and Pătârlagele in Romania, which are dated to Oligocene [17]. Simetite is a characteristic amber deriving from a deposit close to river Simeto, in Sicily, which has been dated to Miocene [14]. Ambers from central Italy have been dated to Oligocene [31]. Information on the geological origin was not available for some of the samples. Before analysis, a small amount of each sample was grinded to a fine powder using a Pulverisette 23 laboratory scale ball mill (Fritsch, Germany). All samples could be easily milled in less than 10 s, and no significant increase in temperature was observed, so that cryo-milling with liquid nitrogen was not necessary.

Table 1
Labels, geological classification, geographical origin, and providers of all amber samples. 1 – Natural History Museum of Warszawa, Poland; 2 – Natural History Museum of Milano, Italy; 3 – The Louvre Museum in Paris, France; 4 – Getty Institute, Los Angeles, USA; 5 – University of Padova, Italy; 6 – Natural History Museum of Calci, Italy; 7 – University of Modena and Reggio Emilia, Italy; 8 – "G. Zannato" Museum of Archaeology and Natural Sciences, Montecchio Maggiore, Italy; 9 – Romanian National History Museum, Bucharest, Romania.

Label	Provider	Classification	Geographical origin
Sg01	1	Siegburgite	Bitterfeld, Germany
Gl01	1	Glessite	Hoyerwerda, Germany
Gl02	1	Glessite	Not provided
Gl03	1	Glessite	Not provided
Ge01	1	Gedanite	Bitterfeld, Germany
Ge02	1	Gedanite	Mikoszewo, Poland
GS01	1	Gedano-succinite	Pomerania, Poland
Go01	1	Goitschite	Bitterfeld, Germany
Go02	1	Goitschite	Not provided
BA01	1	Black amber	Bitterfeld, Germany
BA02	1	Black amber	Bitterfeld, Germany
BA03	1	Black amber	Ukraine
BA04	1	Black amber	Poland
Su01	1	Succinite	Bitterfeld, Germany
Su02	1	Succinite	Bitterfeld, Germany
Su03	1	Succinite	Klesow, Ukraine
Su04	1	Succinite	Klesow, Ukraine
Su05	1	Succinite	Jantarnyj, Russia
Su06	2	Succinite	Not provided
Su07	2	Succinite	Not provided
Su08	2	Succinite	Not provided
Su09	2	Succinite	Not provided
Su10	2	Succinite	Not provided
Su11	3	Succinite	Not provided
Su12	3	Succinite	Not provided
Su13	3	Succinite	Not provided
Su14	3	Succinite	Not provided
Su15	4	Succinite	Not provided
Su16	4	Succinite	Not provided
Su17	5	Succinite	Russia
Su18	5	Succinite	Gdańsk – Stogi, Poland
Su19	5	Succinite	Bitterfeld, Germany
CI01	6	Unknown	Scannello, Italy
CI02	7	Unknown	Loiano, Italy
CI03	7	Unknown	Prignano, Italy
Si01	8	Simetite	Sicily, Italy
Si02	8	Simetite	Sicily, Italy
Ru01	9	Rumanite	Colți, Romania
Ru02	9	Rumanite	Colți – Pătârlagele, Romania
Ru03	9	Rumanite	Colți – Pătârlagele, Romania
Ru04	9	Rumanite	Colți – Pătârlagele, Romania
Ru05	9	Rumanite	Colți – Pătârlagele, Romania
Ru06	9	Rumanite	Sibiciu de Jos, Romania
Ru07	9	Rumanite	Colți – Pătârlagele, Romania
Ru08	9	Rumanite	Colți – Buzău, Romania
Ru09	9	Rumanite	Colți – Buzău, Romania

2.2. Evolved gas analysis-mass spectrometry (EGA-MS)

Experiments were performed with an EGA/PY-3030D microfurnace pyrolyzer (Frontier Laboratories, Japan) coupled to a 6890 gas chromatograph and a 5973 mass spectrometric detector (Agilent Technologies, USA). In each experiment, approximately 100 μg of sample were directly weighted in the sample holder and inserted in the pyrolysis furnace. The temperature of the furnace was then raised from 50 °C to 700 °C at 10 °C/min. The temperature of the pyrolysis interface was kept 100 °C above the furnace temperature, up to a maximum of 300 °C. Injection was performed in split mode at 280 °C with a 20:1 ratio. Desorption/pyrolysis products are directly sent to the MS detector through an UADTM-2.5 N deactivated stainless steel capillary tube (Frontier Laboratories, Japan) at 300 °C. Helium (1 mL min^{-1}) was used as carrier gas. The mass spectrometer was operated in EI positive mode (70 eV). The observed m/z range was 50 – 800. Values below m/z 50 are generally poorly diagnostic, and their detection was avoided. The ion source and quadrupole analyzer were at 230 °C and 150 °C, respectively.

2.3. Data processing

EGA-MS profiles were processed with MassHunter (ver. 10.0, Agilent Technologies, USA). Mass spectra were interpreted by comparison with those available in reference libraries (NIST20, NIST, USA) and in previous publications [8,18,32–39]. Reproducibility of the EGA-MS experiments was assessed by repeating the analysis of the same sample three times and calculating the error on the total integrated area of the thermograms divided by the sample weight. The relative standard deviation was 9% on average.

Principal component analysis (PCA) of mass spectral data from succinite, rumanite, gedanite and gedano-succinite samples was performed with OriginPro 2018. The data matrix was built with the average mass spectra of all samples calculated through the whole thermal degradation range. For this data matrix, the *m/z* range was restricted to 50–350 to avoid contribution from the background noise. Two additional PCAs were performed using the average mass spectra calculated in two different temperature ranges: 50–300 °C for the non-polymeric components, and 300–550 °C for the polymeric components. Principal components were always calculated using the covariance matrix.

3. Results and discussion

3.1. Glessites and goitschites

EGA-MS profiles of a representative glessite and goitschite and corresponding average mass spectra are shown in Fig. 1, along with proposed structures for the main *m/z* signals. EGA-MS profiles of all samples are available in the Supplementary Material. The two amber types displayed similar thermal and mass spectral features. We identified three main gas evolution regions in all Gl and Go samples (see Table 1 for compound labels): a first region between 100 and 200 °C, a second region between 200 and 300 °C, and a third region between 300 and 550 °C. The third region showed the highest signal intensity in all samples.

High signals at *m/z* 202 and 204 were detected in all three regions of the thermograms. These signals can be ascribed to sesquiterpenoids. Sesquiterpenoids with cadinene-like structures were previously identified in glessite samples by Yamamoto et al. [16]. The main MS fragmentations for cadinenes are the loss of the methyl or the isopropyl group, generating the signals at *m/z* 161, 159, 189, and 187.

The signal at *m/z* 408 can be ascribed to dimeric cadinene. The dimer undergoes the same MS fragmentations of the monomer, with loss of methyl or isopropyl groups giving *m/z* 365 and 393. Cleavage of the C-C

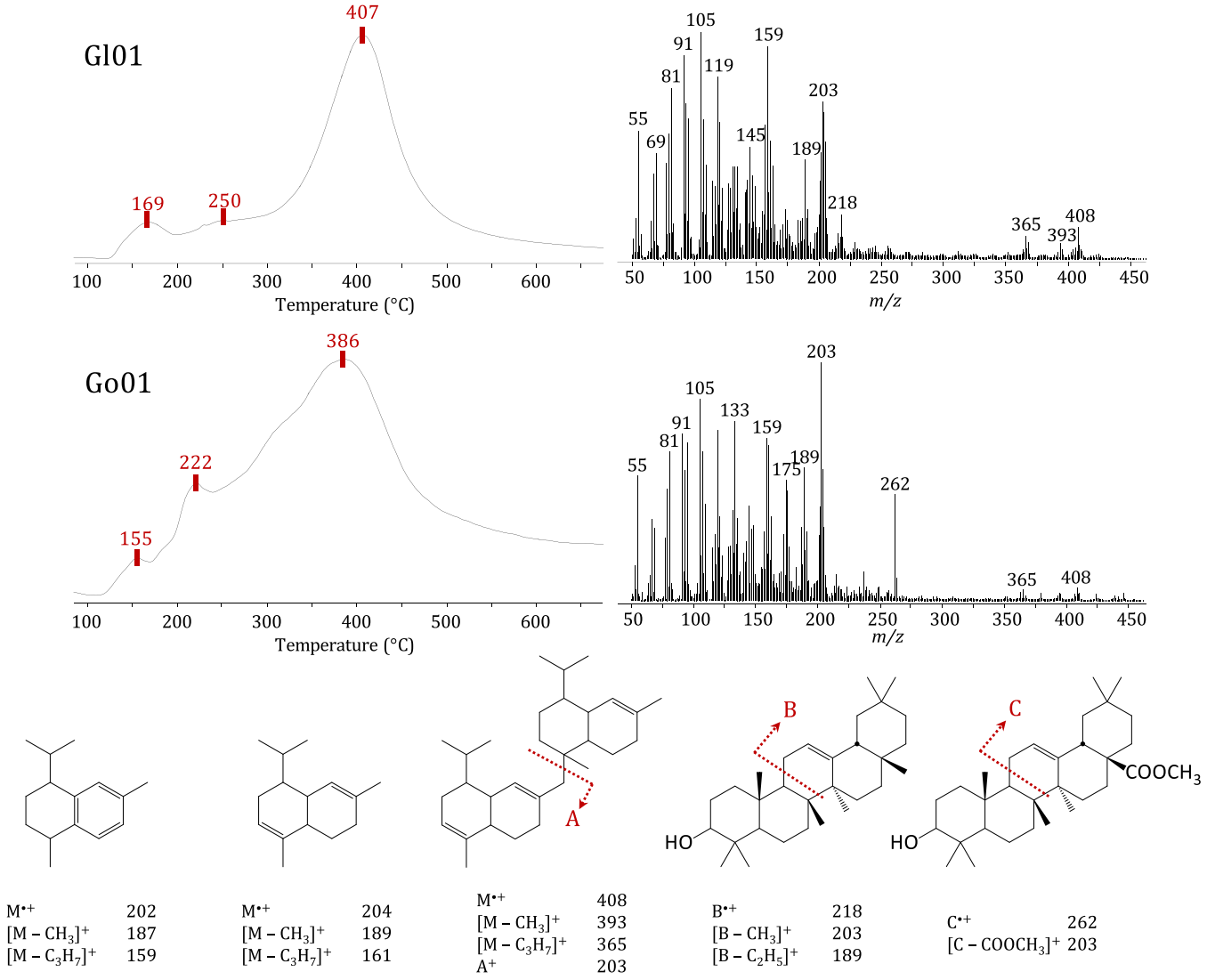

$M^{\bullet+}$	202	$M^{\bullet+}$	204	$M^{\bullet+}$	408	$B^{\bullet+}$	218	$C^{\bullet+}$	262
$[M - CH_3]^+$	187	$[M - CH_3]^+$	189	$[M - CH_3]^+$	393	$[B - CH_3]^+$	203	$[C - COOCH_3]^+$	203
$[M - C_3H_7]^+$	159	$[M - C_3H_7]^+$	161	$[M - C_3H_7]^+$	365	$[B - C_2H_5]^+$	189		
				A^+	203				

Fig. 1. EGA-MS profiles and average mass spectra for samples Gl01 (glessite) and Go01 (goitschite). Proposed structures of ions for *m/z* signals of relevance are also shown.

bond between the two sesquiterpene units is also possible, generating *m/z* 203. The signal at *m/z* 203 can be observed in both the second and third region of the thermogram, indicating that higher cadinene oligomers and polymers are also present in Gl and Go samples. Oligomeric and polymeric cadinenes have been observed in both fresh and fossil triterpenoid resins [34,40].

Additional signals were detected in the mass spectra of the second and third regions. Glessite samples showed high intensity of *m/z* 218, while goitschite samples showed high intensity of *m/z* 262. The even values indicate that the corresponding structures are obtained by rearrangement reactions. The most common rearrangement in terpenes is the retro-Diels-Alder (RDA) elimination. The formation of ions with *m/z* 218 and 262 through RDA of triterpenes has been documented in the papers by Djerassi and co-workers [32,33]. As triterpenes were detected in previous studies of glessites [16], we hypothesize that triterpenes are also present in our glessites and goitschites. The different *m/z* values indicate that Gl and Go samples contain triterpenoids with different structures. In particular, *m/z* 218 can be ascribed to triterpene hydrocarbons with the ursane and oleanane structures, such as α- and β-amyrin, while *m/z* 262 can be obtained from the methyl carboxylate equivalents of the same compounds. Note that additional MS fragmentations of these ion radicals can also generate *m/z* 189 and 203, as suggested in Fig. 1.

The trends of the discussed *m/z* signals in the three gas evolution regions can be used to outline a general picture of the thermal behavior of Gl and Go ambers. The two amber types contain both monomeric and oligo/polymeric sesquiterpenes, most likely with the cadinene carbon skeleton. In addition, glessites also contain amyrin-like triterpenoids, while goitschites contain triterpenoids with ursane or oleanane structures bearing a methyl-carboxylate functional group, most likely located on carbon 28. These results allow us to identify both Gl and Go ambers as class II ambers [6].

The results obtained for goitschites in this study are in disagreement with those of the study by Yamamoto and co-workers [16], which reported the presence of diterpenoids in a goitschite sample with the same geographical origin as sample Go01. This significant difference in results highlights that the geological denomination of an amber sample should always be supported by information on its molecular composition. Different results obtained from the characterization of ambers with the same geological name are not necessarily ascribable to poorly conducted experiments or mislabeling of the samples. Rather, geological denomination of amber samples is often based on their geographical origin or physical and optical features, without information on its molecular composition. This is especially true for ambers which entered museum and academic collections in the previous century, when instrumental analytical techniques were far less available [31].

3.2. Siegburgite and black ambers

EGA-MS profiles for sample Sg01 and a representative black amber sample are shown in Fig. 2. Sample Sg01 was the only instance of polystyrene-like amber in the sample pool. Polystyrene-like ambers belong to class III [10,41]. This peculiar type of amber has been documented since the 19th century [42]. Grimaldi and co-workers gave a thorough account of polystyrene-like amber slabs found in New Jersey, but this type of amber was also found in the Bitterfeld deposit [43,44].

The average mass spectrum for this sample showed the characteristic *m/z* signals ascribable to polystyrene [35]. The sample showed a single gas evolution region, with a signal peak at 405 °C. The high temperature value indicates that the gas evolution peak corresponds to a thermal

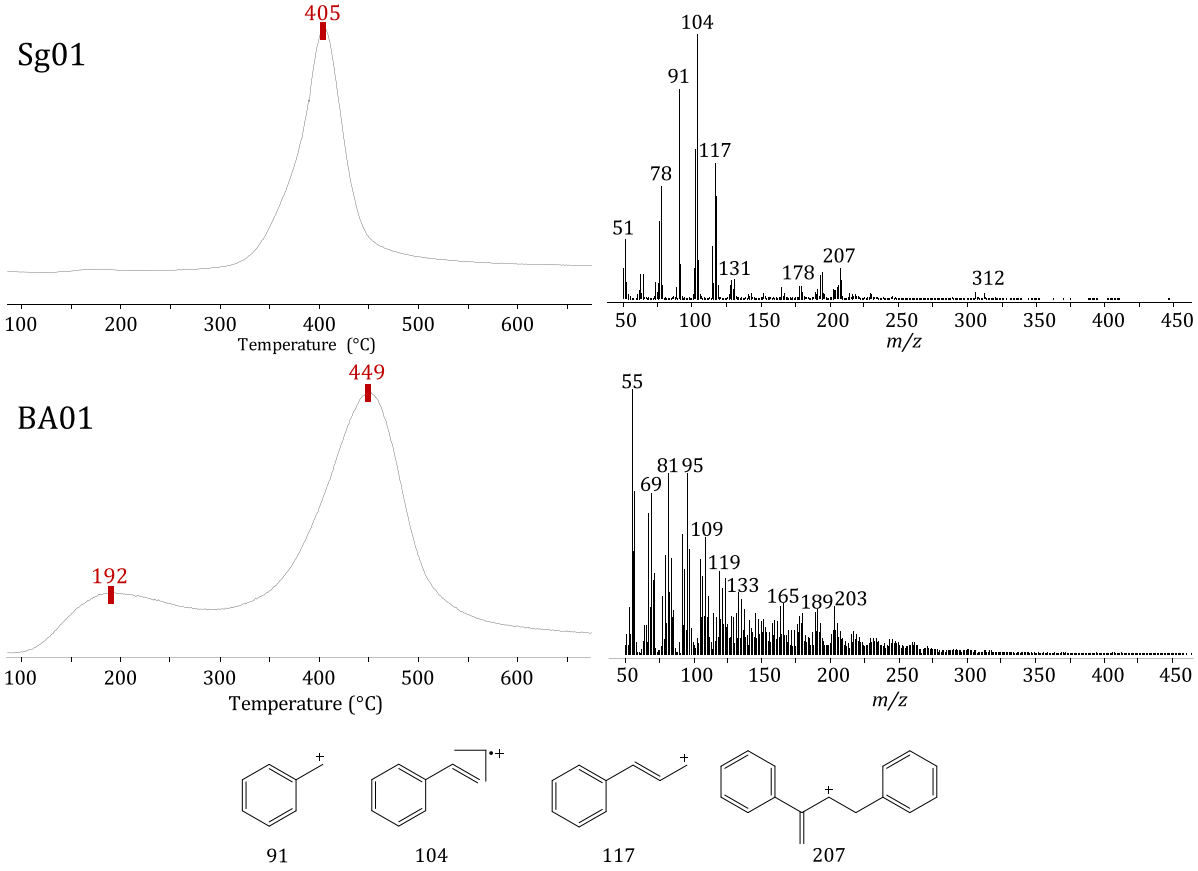

Fig. 2. EGA-MS profiles and average mass spectra for samples Sg01 (siegburgite) and BA01 (stantienite). Proposed structures of ions for *m/z* signals of relevance in sample Sg01 are also shown.

degradation of the polymeric bulk of the material, and that sample Sg01 contains very small amounts of non-polymeric species. While polystyrene represents the bulk of the sample, the presence of oxygenated species in siegburgite has also been reported. These species are mainly cinnamic acid and its esters, which have been proven to act as cross-linkers in the polymeric network [41]. These compounds are most likely related to the original components of the resin. The most probable botanical origin for this amber is in fact the liquidambar plant (*Altingiaceae* family), whose resin has a high content of cinnamic acid and its esters [45]. Upon pyrolysis, these oxygenated species generate cinnamic acid derivatives such as 3-phenylpropanylcinnamate, which has been proposed by Pastorova and co-workers as a marker to distinguish siegburgite from New Jersey class III amber and from synthetic polystyrene [41]. The mass spectrum of 3-phenylpropanylcinnamate shows a signal at *m/z* 118 as base peak. The relative intensity of *m/z* 118 in sample Sg01 is indeed higher than what is usually observed for synthetic polystyrene. However, *m/z* 118 can also be ascribed to methylstyrene, which is also a pyrolysis product of polystyrene [35]. Therefore, no definitive conclusion on the authenticity or the botanical origin of this sample can be drawn based on EGA-MS analyses alone.

Black amber is also known as stantienite [16]. Contrary to siegburgite, the EGA-MS profiles of all black ambers showed two main gas evolution regions: a first region in the range 100 – 300 °C, and a second region in the range 300 – 600 °C. Interpretation of the mass spectra of BA samples was not straightforward, as the highest signals throughout the thermogram were at low *m/z* values (below *m/z* 150), which are poorly diagnostic. However, three series of signals can be outlined, corresponding to saturated (*m/z* 57, 71, 85), mono-unsaturated (*m/z* 55, 69, 83, 97, 111), and di-unsaturated (*m/z* 67, 81, 95, 109, 123) linear aliphatic hydrocarbons. These signals were present with little variations in relative intensity throughout the EGA-MS profile, indicating that linear hydrocarbons are the main components of both the non-polymeric and polymeric fractions of black ambers. This indicates that black ambers underwent extensive maturation, and are almost completely fossilized.

Yamamoto and co-workers [16] identified two homolog series of methyl esters of mono- and dicarboxylic fatty acids in dichloromethane: methanol extracts of a stantienite sample. Both categories of compounds share *m/z* 74 as a very intense signal in their mass spectra. However, this signal was not found in any of the BA samples of our study, suggesting that our black amber samples are either at a more advanced state of maturation, or that their content of these methyl esters is extremely low. The amount of methyl esters in the stantienite sample of Yamamoto is not known, as no quantitative information is provided in the paper.

3.3. Succinite, rumanite, gedanite and gedano-succinite

EGA-MS profiles and average mass spectra for these four types of amber are presented in Fig. 3. All Su, Ru, Ge and GS samples showed two gas evolution regions in the temperature ranges 100 – 300 °C and 300 – 550 °C. As observed for the other amber types, these regions can be ascribed to desorption of non-polymeric compounds at low temperatures, and to the pyrolysis of the polymeric matrix above 300 °C. While this behavior is shared by all samples, the two gas evolution regions displayed different profiles. For instance, gedanites and gedano-succinites provided gas evolution regions with multiple signal peaks both in the thermal desorption and the pyrolysis ranges, while most succinites and rumanites provided a single peak in either range.

Interpretation of the mass spectra of these samples was based on the results of previous studies dealing with succinite and rumanite [8,17,18,24], and on studies dealing with the interpretation of mass spectra of diterpenes [36,37]. The thermal desorption region of all samples showed high signals of *m/z* 95, 119 and 134. The signal at *m/z* 95 can be ascribed to camphene-like monoterpenoids, such as borneol and camphor, while those at *m/z* 119 and 134 can be ascribed to aromatic monoterpenes such as *p*-cymene. Structures for these compounds are shown in Fig. 3. All these compounds were detected in the volatile fraction of rumanite and succinite samples by SPME [17]. Gedanite and gedano-succinite samples showed additional signals at *m/z* 241, 257, 287, 302, with peaks at approximately 240 °C. These signals can be ascribed to diterpenoid acids. A survey of the mass spectra of diterpenoid acids available in the literature and in the NIST library showed that the abietane, pimarane and isopimarane structures are the most likely to be present in Ge and GS samples. The signal at *m/z* 302 corresponds to the molecular ion of abietic/pimaric/isopimaric acid, while the other signals can be ascribed to ions obtained by characteristic fragmentation patterns, such as the loss of methyl radical or decarboxylation.

The second gas evolution region showed very complex mass spectra in all samples. Discussion of this region of the thermogram is particularly challenging, as the signals with the highest intensities were at relatively low *m/z* values, which are poorly diagnostic. Compared to the first gas evolution region, higher relative intensities were observed for *m/z* 173, 175, 177, 189 and 191. These signals can be ascribed to the bicyclic pyrolysis products of the poly-labdanoid polymeric network which is known to be the main constituent of the bulk of succinite and rumanite ambers [8]. The same signals were found in gedanite and gedano-succinite, indicating that these samples also share a similar composition of the polymeric fraction. The mass spectra of both gas evolution regions demonstrate that Su, Ru, Ge and GS samples all share very similar compositional profiles. This is in agreement with results available in the literature, which ascribe all these amber varieties to a common botanical source [8,39], and allows us to assign all samples to class I. Class I contains a range of subclasses with significantly different molecular composition. A pivotal discrimination criterion among these subclasses is the presence and amount of succinic acid, which can be found for instance in subclass Ia, and Id ambers, but not in subclasses Ib and Ic [6]. Succinic acid in amber can be found in amounts as high as 8% [39], and can be both a component of the non-polymeric fraction, and part of the polymeric matrix, forming ester bonds with hydroxy groups on polymerized terpenoids [46]. Free succinic acid can be converted in the corresponding anhydride during heating [47,48]. However, both succinic acid and succinic anhydride show high signals at low *m/z* values, which are poorly diagnostic as they can also be ascribed to numerous fragmentations of the terpenoid components. Detection of the terpenoid-succinic acid esters is also challenging, as their main fragment ions are the same of non-esterified terpenoids [46]. Therefore, detection of succinic acid or its derivatives in EGA-MS profiles was not possible, and we avoided assigning the samples to specific subclasses.

As Su, Ru, Ge and GS ambers all provided similar gas evolution profiles, principal component analysis (PCA) was performed to highlight differences between the four types. Average mass spectra in the range *m/z* 50 – 300 and 100 – 550 °C were used as data matrix. The results are presented in Fig. 4. The first two principal components accounted for approximately 75% of the total variance. The most interesting discrimination of the samples was along the first principal component, in which all rumanite samples were at negative values, and all succinite, gedanite and gedano-succinite samples were at positive values. The loading plot of the first principal component, also shown in Fig. 4, indicates that *m/z* 55, 57, 69 and 83 are the main signals pulling samples towards negative values. While not diagnostic, these *m/z* signals can be ascribed to small hydrocarbon fragment ions deriving from the terpenes of both the non-polymeric and polymeric fractions of amber. The results of the PCA indicates that rumanite samples have higher relative intensities of these signals. This suggests that rumanite has a higher content of defunctionalized terpenes, and a lower content of oxygenated functional groups. This result is consistent with the findings of Stout and co-workers [8], who identified rumanite as a variety of succinite amber which underwent a partial thermal degradation, accelerating the maturation process of amber and favoring defunctionalization and the loss of hydroxy and carboxy groups. Exposure to high temperatures also likely favored the loss of low-molecular weight components from the bulk of the amber. This hypothesis is supported in our results by the

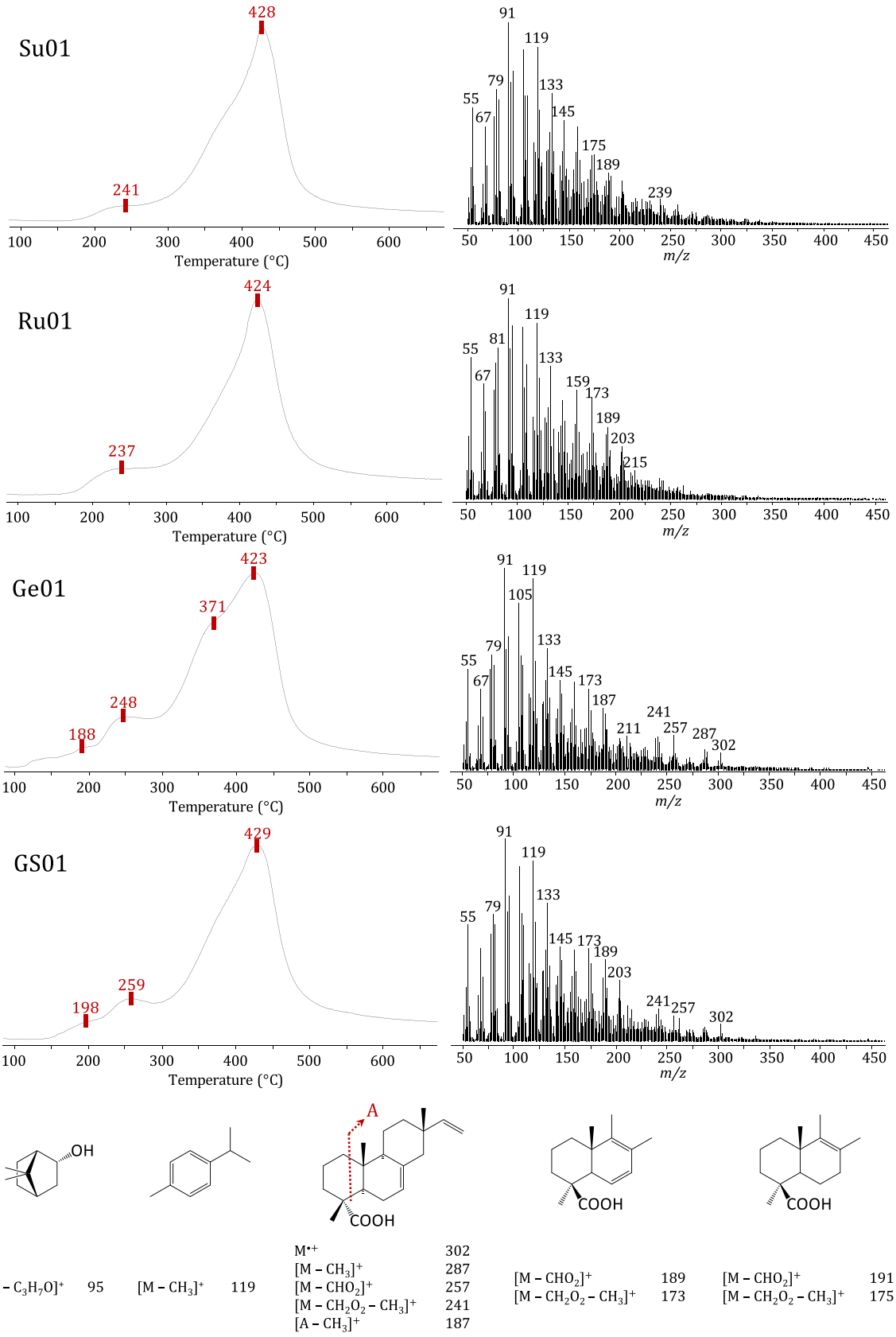

$[M - C_3H_7O]^+$	95	$[M - CH_3]^+$	119	$M^{\bullet+}$	302	$[M - CHO_2]^+$	189	$[M - CHO_2]^+$	191
				$[M - CH_3]^+$	287	$[M - CH_2O_2 - CH_3]^+$	173	$[M - CH_2O_2 - CH_3]^+$	175
				$[M - CHO_2]^+$	257				
				$[M - CH_2O_2 - CH_3]^+$	241				
				$[A - CH_3]^+$	187				

Fig. 3. EGA-MS profiles and average mass spectra for samples Su01 (succinite), Ru01 (rumanite), Ge01 (gedanite) and GS01 (gedano-succinite). Proposed structures of ions for *m/z* signals of relevance are also shown.

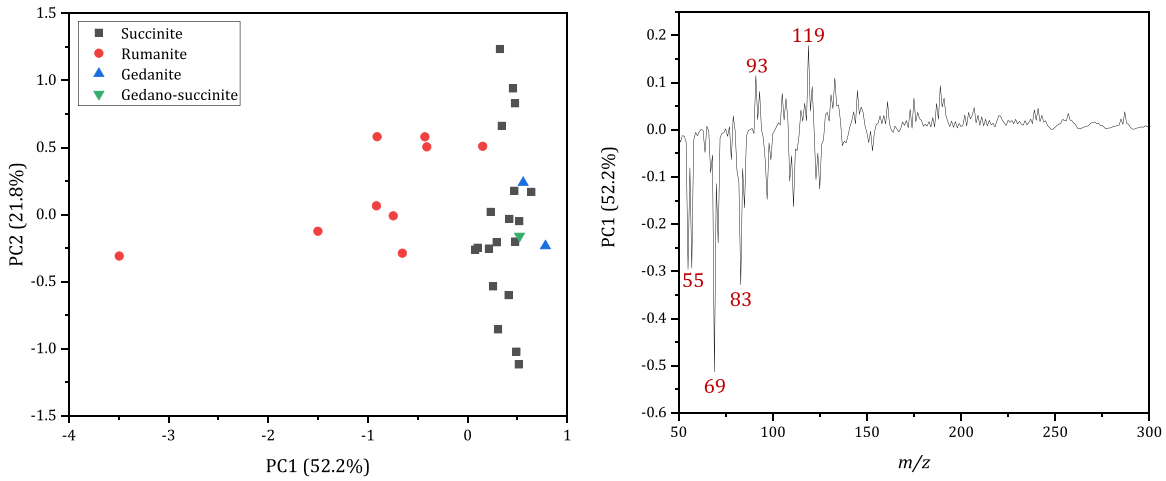

Fig. 4. Left – Score plot of the first two principal components of Su, Ru, Ge and GS samples. Right – Loading plot of the first principal component.

loading of *m/z* 119, which pulls samples towards positive values of the PC1. As *m/z* 119 can be ascribed to monoterpenes, the results of the PCA suggest that succinite, gedanite and gedano-succinite samples have a higher content of low-molecular weight compounds than rumanite.

PCA was also repeated using average mass spectra obtained either from the thermal desorption region (100 – 300 °C) or from the pyrolysis region (300 – 550 °C) of the thermogram. The resulting score and loading plots are available in the Supplementary Material. Interestingly, both additional PCAs provided very similar results to those obtained with the first one. This indicates that the compositional differences between rumanite and succinite/gedanite/gedano-succinite involve both the non-polymeric and polymeric fractions. When considering MS signals from the thermal desorption region, a high load of *m/z* 119 was obtained pulling samples towards negative values of PC1, and Su, Ge and GS samples were found at negative PC1 scores. This suggests that these samples have a higher content of cymene-like monoterpenoids, which are the main responsible for the signal at *m/z* 119 in the thermal desorption region. This is in agreement with the results obtained by van der Werf and co-workers [17], in which PCA of SPME chromatograms also showed that Baltic amber contains more cymene terpenoids than rumanite.

Note that succinite, gedanite and gedano-succinite could not be separated from each other, even along the other principal components. This indicates that the compositional differences between these three types of amber are small in comparison with the differences from rumanite samples. We avoided repeating PCA on Su, Ge and GS ambers as the number of samples is not sufficient to draw statistically significant conclusions. To attempt discrimination of gedanite and gedano-succinite, principal component analysis was also repeated using normalized total ion currents instead of the average mass spectra, but no further discrimination was obtained.

3.4. Italian ambers

EGA-MS profiles for samples Si01 and CI01–03 are shown in Fig. 5. Sicilian amber has been documented in a previous study by van der Werf and co-workers [38]. Py-GC/MS analysis of this amber provided mostly diterpenes with the enantio-biformene carbon skeleton, as well as bicyclic compounds deriving from the pyrolysis of these diterpenes. The characteristic *m/z* signals of these compounds were also detected in the mass spectra of both simetite samples in this study. High relative intensities of *m/z* 245 and 260 were observed in the thermal desorption region. These signals can be ascribed to biformene-like diterpenes with 19 carbon atoms, which were found in significant amounts in the study by van der Werf and co-workers. A representative structure for one of these compounds is shown in Fig. 5. Interestingly, the relative intensity of *m/z* 119 in these samples was lower than those observed in the other diterpenoid ambers, indicating a low content of aromatic monoterpenes.

Pyrolysis of the polymeric fraction of Sicilian ambers showed very similar signals to those observed for the ambers described in Section 3.3, leading us to the conclusion that the macromolecular network is mainly constituted of polymeric labdane terpenoids. Our results are in agreement with the findings of van der Werf [38] that this polymeric network is composed of biformene-like labdane, reflecting the composition of the non-polymeric fraction, and that Sicilian ambers can be ascribed to class Ic.

Samples CI01–03 were obtained from central Italy. Two literature studies are available describing ambers from this region [31,49], including a work by van der Werf in which Py-GC/MS was performed on a sample with the same geological origin as sample CI03. As most of the other samples, CI ambers showed two thermal degradation regions. In the first region, all samples showed high signals at *m/z* 119, 159, and 173. Samples CI02 and CI03 also showed high intensities of *m/z* 95.

Signals at *m/z* 95 and 119 can be ascribed to fragment ions of octahydronaphthalenes, while signals at *m/z* 159 and 173 can be ascribed to tetrahydronaphthalenes with one aromatic and one aliphatic ring. These species are found in class I ambers as a result of defunctionalization and loss of the aliphatic side-chain of labdanoid diterpenes [50]. Octahydronaphthalenes were indeed found in the study by van der Werf [31]. Representative structures of tetrahydro- and octahydronaphthalenes are shown in Fig. 5 to account for these signals. Sample CI02 also showed the same signals at *m/z* 245 and 260 that were found in the Sicilian ambers. This led us to the conclusion that sample CI02 is also constituted of biformene terpenoids. A high relative intensity was also observed for *m/z* 231 in CI02. While this signal is not characteristic of biformene-like terpenoids, unidentified compounds with this signal were detected in Py-GC/MS of Sicilian amber [38].

Finally, all three samples provided very similar mass spectra in the pyrolysis region. These mass spectra were like those obtained for Sicilian ambers and the other diterpenoid ambers, suggesting the presence of a labdanoid-based polymeric network. For this reason, all CI samples were also ascribed to class I. This also agrees with the results obtained by van der Werf [31]. Table 2 provides a synthetic report of the classes and main components of both non-polymeric and polymeric fractions for all amber samples in this study.

4. Conclusions

Gas evolution profiles of almost all ambers showed two main regions, which could be ascribed to the desorption of low-molecular weight compounds at low temperatures, and to the pyrolysis of the polymeric network above 300 °C. Samples with different geological origin

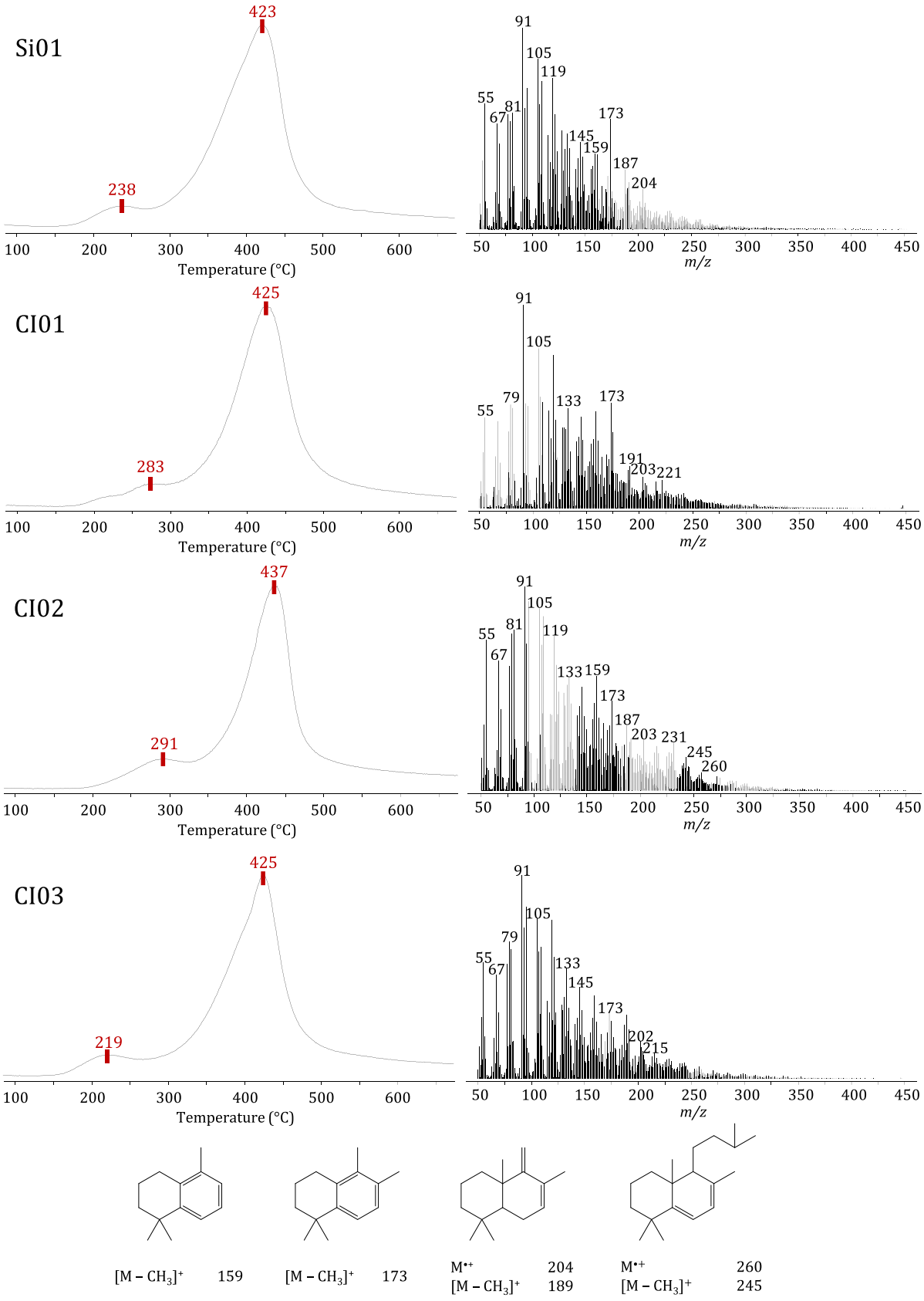

Fig. 5. EGA-MS profiles and average mass spectra for samples Si01 (simetite) and CI01–03 (ambers from central Italy). Proposed structures of ions for *m/z* signals of relevance are also shown.

Table 2
Classes and composition of the non-polymeric and polymeric fractions of all amber samples in this study, based on EGA-MS results.

Amber type	Class	Non-polymeric fraction (< 300 °C)	Polymeric fraction (> 300 °C)
Glessite	II	Cadinene-like sesquiterpenes Ursane/oleanane-like triterpenes	Polymeric cadinenes
Goitschite	II	Cadinene-like sesquiterpenes Ursane/oleanane-like triterpenes with methyl-carboxylates on C28	Polymeric cadinenes
Siegburgite	III	-	Polystyrene, possibly with oxygenated cross-linkers
Black amber	-	Aliphatic hydrocarbons	Aliphatic hydrocarbons
Succinite	I	Camphene-like monoterpenoids Cymene-like monoterpenoids	Polylabdene
Rumanite	I	Camphene-like monoterpenoids Cymene-like monoterpenoids	Polylabdene
Gedanite	I	Camphene-like monoterpenoids Cymene-like monoterpenoids Pimarane-like diterpenoid acids	Polylabdene
Gedano-succinite	I	Pimarane-like diterpenoid acids	Polylabdene
Simetite	I	Biformene-like diterpenoids	Polylabdene
CI01	I	Tetrahydronaphthalenes	Polylabdene
CI02	I	Tetrahydronaphthalenes Octahydronaphthalenes Biformene-like diterpenoids	Polylabdene
CI03	I	Tetrahydronaphthalenes Octahydronaphthalenes	Polylabdene

generally showed different desorption/pyrolysis temperatures and different number of desorption peaks, highlighting the usefulness of EGA-MS in providing information for the development of Py-GC/MS experiments targeting different fractions of specific amber samples.

EGA-MS provided valuable information on the thermal behavior of all amber samples, and on their content of non-polymeric and polymeric components. The results allowed us to attribute a class to most of the samples. These classes were in agreement with those attributed in previous literature studies dealing with ambers with same geological origins, with the only exception of the goitschites, which were identified as triterpenoid ambers and not diterpenoid. The two types of class II ambers, glessite and goitschite, could be distinguished based on the different constituting triterpenoids. Distinction of succinite and rumanite samples was also possible by principal component analysis of their average mass spectra.

For ambers of class I, subclasses could not be attributed due to the inability to detect the presence of succinic acid or to pinpoint specific terpenoid structures. This highlights a constraint of EGA-MS results, which is the lack of chromatographic separation of the desorption/pyrolysis products. For this reason, additional characterization with Py-GC/MS techniques should be performed on the sample pool. A particularly promising approach would be the use of step-wise Py-GC/MS, which could be achieved by sequentially heating an amber sample at two different temperatures, in order to achieve the desorption of the non-polymeric fraction, followed by the pyrolysis of the residual polymeric fraction. For such a study, the choice of desorption/pyrolysis temperatures would be guided by the EGA-MS results obtained in this work.

CRediT authorship contribution statement

Marco Mattonai: Conceptualization, Methodology, Software, Formal analysis, Investigation, Data curation, Writing – original draft, Writing – review & editing, Visualization. **Lucia Andrei:** Methodology, Software, Validation, Formal analysis, Investigation, Data curation. **Marian Vîrgolici:** Resources. **Erika Ribechini:** Conceptualization, Resources, Writing – original draft, Supervision, Project administration, Funding acquisition.

Declaration of Competing Interest

The authors declare that they have no known competing financial interests or personal relationships that could have appeared to influence the work reported in this paper.

Data availability

Data will be made available on request.

Acknowledgements

The Authors are deeply grateful to all the institutions for providing the amber samples.

Appendix A. Supporting information

Supplementary data associated with this article can be found in the online version at doi:10.1016/j.jaap.2023.105994.

References

[1] D.A. Grimaldi, Amber in Nature, in H. Whelcher (Ed.), Amber - Window to the Past, Harry N. Abrams, Incorporated, New York, USA, 1996, p. 11.
[2] S. Veil, K. Breest, P. Grootes, M.-J. Nadeau, M. Hüls, A 14 000-year-old amber elk and the origins of northern European art, Antiquity 86 (2012) 660.
[3] M.P. Colombini, E. Ribechini, M. Rocchi, P. Selleri, Analytical pyrolysis with in-situ silylation, Py(HMDS)-GC/MS, for the chemical characterization of archaeological and historical amber objects, Herit. Sci. 1 (2013) 6.
[4] R. Shor, The history and reconstruction of the amber room, Gems Gemol. 54 (2018) 378.
[5] D.J. Clifford, P.G. Hatcher, R.E. Botto, J.V. Muntean, B. Michels, K.B. Anderson, The nature and fate of natural resins in the geosphere—VIII.1For the last publication in this series see Anderson, 1996.1 NMR and Py–GC–MS characterization of soluble labdanoid polymers, isolated from Holocene class I resins, Org. Geochem. 27 (1997) 449.
[6] K.B. Anderson, J.C. Crelling, Introduction, in: K.B. Anderson, J.C. Crelling (Eds.), Amber, Resinite, and Fossil Resin, American Chemical Society, USA, 1995, p. XI.
[7] K.B. Anderson, R.E. Winans, R.E. Botto, The nature and fate of natural resins in the geosphere—II. Identification, classification and nomenclature of resinites, Org. Geochem. 18 (1992) 829.
[8] E.C. Stout, C.W. Beck, K.B. Anderson, Identification of rumanite (Romanian amber) as thermally altered succinite (Baltic amber), Phys. Chem. Miner. 27 (2000) 665.
[9] M.A. Wilson, J.V. Hanna, K.B. Anderson, R.E. Botto, 1H CRAMPS NMR derived hydrogen distributions in various coal macerals, Org. Geochem. 20 (1993) 985.
[10] W. Winkler, M. Musso, E.C. Kirchner, Fourier Transform Raman Spectrosc. data Foss. Resin Siegbg. 34 (2003) 157.
[11] J.B. Lambert, G.O. Poinar, Amber: the Organic Gemstone, *Acc. Chem. Res.* 35 (2002) 628.
[12] A.P. Wolfe, R.C. McKellar, R. Tappert, R.N.S. Sodhi, K. Muehlenbachs, Bitterfeld amber is not Baltic amber: Three geochemical tests and further constraints on the botanical affinities of succinite, Rev. Palaeobot. Palynol. 225 (2016) 21.
[13] C.W. Beck, Spectroscopic Investigations of Amber, Appl. Spectrosc. Rev. 22 (1986) 57.
[14] E. Ragazzi, G. Roghi, A. Giaretta, P. Gianolla, Classification of amber based on thermal analysis, Thermochim. Acta 404 (2003) 43.
[15] M. Feist, I. Lamprecht, F. Müller, Thermal investigations of amber and copal, Thermochim. Acta 458 (2007) 162.
[16] S. Yamamoto, A. Otto, G. Krumbiegel, B.R.T. Simoneit, The natural product biomarkers in succinite, glessite and stantienite ambers from Bitterfeld, Germany, Rev. Palaeobot. Palynol. 140 (2006) 27.
[17] I.D. van der Werf, A. Aresta, G.I. Truică, G.L. Radu, F. Palmisano, L. Sabbatini, A quasi non-destructive approach for amber geological provenance assessment based on head space solid-phase microextraction gas chromatography–mass spectrometry, Talanta 119 (2014) 435.
[18] K.B. Anderson, R.E. Winans, Nature and fate of natural resins in the geosphere. I. Evaluation of pyrolysis-gas chromatography mass spectrometry for the analysis of natural resins and resinites, Anal. Chem. 63 (1991) 2901.
[19] K.B. Anderson, R.E. Botto, The nature and fate of natural resins in the geosphere—III. Re-evaluation of the structure and composition of Highgate Copalite and Glessite, Org. Geochem. 20 (1993) 1027.
[20] J. Poulin, K. Helwig, The characterisation of amber from deposit sites in western and northern Canada, *J. Archaeol. Sci.: Rep.* 7 (2016) 155.
[21] J. Poulin, K. Helwig, Class Id resinite from Canada: A new sub-class containing succinic acid, Org. Geochem. 44 (2012) 37.

[22] O.O. Sonibare, T. Hoffmann, S.F. Foley, Molecular composition and chemotaxonomic aspects of Eocene amber from the Ameki Formation, Nigeria, Org. Geochem. 51 (2012) 55.
[23] J.B. Lambert, J.A. Santiago-Blay, K.B. Anderson, Chem. Signat. Foss. Resins Recent Plant Exudates 47 (2008) 9608.
[24] M. Vîrgolici, C. Ponta, M. Manea, D. Neguţ, M. Cutrubinis, I. Moise, R. Şuvăilă, E. Teodor, C. Sârbu, A. Medvedovici, Thermal desorption/gas chromatography/mass spectrometry approach for characterization of the volatile fraction from amber specimens: A possibility of tracking geological origins, J. Chromatogr. A 1217 (2010) 1977.
[25] F. Nardella, M. Mattonai, E. Ribechini, Evolved gas analysis-mass spectrometry and isoconversional methods for the estimation of component-specific kinetic data in wood pyrolysis, J. Anal. Appl. Pyrolysis 145 (2020), 104725.
[26] A. Bonini, F.M. Vivaldi, E. Herrera, B. Melai, A. Kirchhain, N.V.P. Sajama, M. Mattonai, R. Caprioli, T. Lomonaco, F.D. Francesco, P. Salvo, A Graphenic Biosensor for Real-Time Monitoring of Urea During Dialysis, IEEE Sens. J. 20 (2020) 4571.
[27] M. Mattonai, A. Watanabe, E. Ribechini, Characterization of volatile and non-volatile fractions of spices using evolved gas analysis and multi-shot analytical pyrolysis, Microchem. J. 159 (2020), 105321.
[28] T. Nacci, F. Sabatini, C. Cirrincione, I. Degano, M.P. Colombini, Characterization of textile fibers by means of EGA-MS and Py-GC/MS, J. Anal. Appl. Pyrolysis 165 (2022), 105570.
[29] K. Mänd, K. Muehlenbachs, R.C. McKellar, A.P. Wolfe, K.O. Konhauser, Distinct origins for Rovno and Baltic ambers: Evidence from carbon and hydrogen stable isotopes, Palaeogeogr., Palaeoclimatol., Palaeoecol. 505 (2018) 265.
[30] J.H. Langenheim, Plant Resins, Am. Sci. 78 (1990) 16.
[31] I.D. van der Werf, A. Monno, D. Fico, G. Germinario, G.E. De Benedetto, L. Sabbatini, A multi-analytical approach for the assessment of the provenience of geological amber: the collection of the Earth Sciences Museum of Bari (Italy), Environ. Sci. Pollut. Res. 24 (2017) 2182.
[32] J. Karliner, C. Djerassi, Terpenoids. LVII. Mass Spectral and Nuclear Magnetic Resonance Studies of Pentacyclic Triterpene Hydrocarbons, J. Org. Chem. 31 (1966) 1945.
[33] H. Budzikiewicz, J.M. Wilson, C. Djerassi, Mass spectrometry in structural and stereochemical problems. XXXII. Pentacyclic Triterpenes, *J. Am. Chem. Soc.* 85 (1963) 3688.
[34] B.G.K. Van Aarssen, J.W. de Leeuw, M. Collinson, J.J. Boon, K. Goth, Occurrence of polycadinene in fossil and recent resins, Geochim. Et. Cosmochim. Acta 58 (1994) 223.
[35] S. Tsuge, H. Ohtani, C. Watanabe, Pyrolysis-GC/MS data book of synthetic polymers: pyrograms, thermograms and MS of pyrolyzates, Elsevier,, 2011 (pp).
[36] T.-L. Chang, T.E. Mead, D.F. Zinkel, Mass Spectra diterpene Resin Acid. methyl Este 48 (1971) 455.
[37] H. Audier, S. Bory, M. Fetizon and N.-T.J.BdlscdF. Anh, Spectres de masse de terpenes. 3. Influence des liaisons ethyleniques sur la fragmentation des diterpenes; 1966: 4002.
[38] I.D. van der Werf, D. Fico, G.E. De Benedetto, L. Sabbatini, The molecular composition of Sicilian amber, Microchem. J. 125 (2016) 85.
[39] E.C. Stout, C.W. Beck, B. Kosmowska-Ceranowicz, Gedanite and Gedano-Succinite, in: K.B. Anderson, J.C. Crelling (Eds.), Amber, Resinite, and Fossil Resins, American Chemical Society, USA, 1995, p. 130.
[40] S.A. Stout, *Resin-Derived Hydrocarbons in Fresh and Fossil Dammar Resins and Miocene Rocks and Oils in the Mahakam Delta, Indonesia*, in *Amber, Resinite, and Fossil Resins*, Chapter 3, American Chemical Society,, 1996, p. 43.
[41] I. Pastorova, T. Weeding, J.J. Boon, 3-Phenylpropanylcinnamate, a copolymer unit in Siegburgite fossil resin: a proposed marker for the Hammamelidaceae, Org. Geochem. 29 (1998) 1381.
[42] H. Klinger, R. Pitschki, Ueber den Siegburgit, *Ber. der Dtsch. Chem. Ges. zu Berl.* 17 (1884) 2742.
[43] D.A. Grimaldi, C.W. Beck, J.J. Boon, Occurrence, chemical characteristics, and paleontology of the fossil resins from New Jersey, Am. Mus. Novit. 2948 (1989) 1.
[44] B.K. Kosmowska-Ceranowicz, G. Bursztyn, Bitterfeldski (saksonski) i inne zywice kopalne z okolic Halle, Prz. Geol. 9 (1990) 394.
[45] M. Hovaneissian, P. Archier, C. Mathe, G. Culioli and C. Vieillescazes, Analytical investigation of styrax and benzoin balsams by HPLC- PAD-fluorimetry and GC-MS; 19, 2008: 301.
[46] J. Poulin, K. Helwig, Inside Amber: The Structural Role of Succinic Acid in Class Ia and Class Id Resinite, Anal. Chem. 86 (2014) 7428.
[47] G.C. Galletti and R. Mazzeo, Pyrolysis/gas chromatography/mass spectrometry and Fourier-transform infrared spectroscopy of amber; 7, 1993: 646.
[48] A.M. Shedrinsky, T.P. Wampler, K.V. Chugunov, The examination of amber beads from the collection of the state hermitage museum found in Arzhan-2 burial memorial site, J. Anal. Appl. Pyrolysis 71 (2004) 69.
[49] I. Angelini, P. Bellintani, Archaeological ambers from northern Italy: an FTIR-DRIFT study of provenance by comparison with the geological amber database, Archaeometry 47 (2005) 441.
[50] K.B. Anderson, New Evidence Concerning the Structure, Composition, and Maturation of Class I (Polylabdanoid) Resinites, in: K.B. Anderson, J.C. Crelling (Eds.), *Amber, Resinite, and Fossil Resins*, American Chemical Society, USA, 1995, p. 105.